Articles in PresS. J Neurophysiol (June 12, 2013). doi:10.1152/jn.00353.2012

TITLE

State-dependence of adaptation of force output following movement observation

AUTHORS

Paul A. Wanda, Gang Li, and Kurt A. Thoroughman

AFFILIATION

Department of Biomedical Engineering, Washington University in Saint Louis, Saint Louis, Missouri, USA.

RUNNING TITLE

Adaptation of force output following observation

CONTACT INFORMATION

Kurt A. Thoroughman

1 Brookings Drive, Campus Box 1097

Saint Louis, Missouri 63130

314-935-9094

thoroughman@biomed.wustl.edu

ABSTRACT

Humans readily learn to move through direct physical practice and by watching the movements of others. Some researchers have proposed that action observation can inform subsequent changes in control through the acquisition of a neural representation of the novel dynamics, but to date, learning following observation has been described by kinematic metrics. Here, we designed an experiment to consider the specificity of adaptation to novel dynamic perturbations at the level of force generation. We measured changes in temporal patterns of force output following either the performance or observation of movements perturbed by either position- or velocity-dependent dynamic environments to (1) establish whether previously described observational motor learning effects were attributable to changes in predictive limb control and (2) determine whether such adaptation reflected a learned dependence on limb states appropriate to the haptic environment. We found that subjects who observed perturbed movements produced significant compensatory changes in their lateral force output, despite never directly experiencing force perturbations firsthand while performing the motor task. The time series of observers' adapted force outputs suggested that the state-dependence of observed dynamics shape adaptation. We conclude that the brain can transform observation of kinematics into state-dependent adaptation of reach dynamics.

KEYWORDS

motor control

force channels

action observation

human motor adaptation

haptic environments

INTRODUCTION

People can learn new motor skills through physical practice and by observing the movements of others. As our bodies fatigue, age, or suffer injury and as we interact with a changing environment, the dynamics of movement are altered, and as a result, constant motor adaptation is necessary to maintain performance. During physical practice of volitional movement, this adaptation is informed by sensory feedback, including vision and proprioception, and the predicted sensory outcomes inferred from neural motor commands (Shadmehr et al. 2010).

When observing the movements of others, people lack this full range of sensory feedback and neural activity associated with generating one's own movement; any adaptive processes must be informed through vision alone. While visual information informs higher-level concepts that affect motor planning and goal-selection**,** movement observation has been shown to induce formation of motor memories that bias evoked force outputs towards replicating the kinematics of the observed actions (Stefan et al. 2005) or aid in moving in novel environment dynamics (Mattar and Gribble 2005). Mattar and Gribble (2005) found that naive observers who watched another person performing a series of point-to-point reaching movements in an unknown dynamic environment performed better (or worse) than non-observing controls when later experiencing and adapting to the same (or opposite) dynamic environment themselves. While subsequent studies replicated and expanded upon this effect (Brown et al. 2009;

Brown et al. 2010), these studies queried learning by measuring changes in kinematic performance during exposure to dynamic perturbations; leaving unclear whether learning by observing builds knowledge of kinematics or dynamics.

In studies of motor control and learning, researchers have examined the adaptation of point-to-point reaching movements to various external loads including robot-generated force field environments. Initially, the unlearned dynamics of these novel body-object interactions cause movement errors. The neural representations of body and environment dynamics may be described as internal models (Kawato 1999), a flexible sensorimotor map. During physical practice, new mappings accounting for the novel external loads are learned, and movements become increasingly accurate (Lackner and Dizio 1994; Shadmehr and Mussa-Ivaldi 1994) as people incrementally modify their temporal patterns of muscular activation (Thoroughman and Shadmehr 1999) to compensate for the novel limb dynamics imposed by the environment. Through the careful design of psychophysical studies and models of learning, some have suggested that the acquisition and modification of internal models takes place through the training of a network of motor primitives whose activity depends upon kinematic signals such as position and velocity (Thoroughman and Shadmehr 2000; Sing et al. 2009). Although adaptation has been typically quantified by kinematic performance metrics (Donchin et al. 2003; Hwang et al. 2003; Thoroughman and Taylor 2005), such as displacement errors during training or after-effects during perturbation-absent washout periods or individual "catch" trials, kinematic metrics

95 reveal the outcome of haptic learning rather than directly assaying the forces
96 people generate.

97 Another assay, the force channel, or error clamp, (Scheidt et al. 2000)
98 directly reads out generated lateral forces and allows researchers to measure
99 predictive force output (Sing et al. 2009; Smith et al. 2006; Hwang et al. 2006;
100 Wagner and Smith 2008; Wei et al. 2010). Sing et al. (2009) measured subjects'
101 force output when adapting to various state-dependent force field environments
102 and found that force production progressed from an initial stereotyped joint-
103 dependence on kinematic limb states, such as position and velocity, to a stronger
104 dependence on the perturbation-relevant limb state (i.e. velocity when adapting
105 to a viscous force field) during training.

106 Here, we asked whether previously-described learning effects of
107 prolonged movement observation (Mattar and Gribble 2005) could be attributed,
108 at least in part, to changes in predictive generation of forces. We were especially
109 motivated to determine whether visually-sensed, kinematic information from
110 observation was truly transformed into an adaptation of dynamic force output,
111 which previous studies were not capable of showing. We designed an
112 experimental paradigm that allowed us to evaluate not only the direction and
113 magnitude of adaptation following observation, but allow us to consider the
114 temporal pattern, or shape, of force output, by using force channel movements to
115 probe adaptation as changes in lateral force output. By training subjects in either
116 position-dependent or velocity-dependent force fields, we further tested whether
117 changes in the temporal pattern of lateral forces differentially reflected the novel

state-force mapping of the observed force field, as typically seen following physical practice.

MATERIALS AND METHODS

A total of 50 neurologically normal, right-handed, human volunteers (20 male, 30 female), aged 18-38, were recruited from the Washington University in St. Louis community to participate in a one-hour, single-day study. Subject handedness was evaluated using the Edinburgh inventory (Oldfield 1971). The experimental protocol was approved by the Washington University Hilltop Human Studies Committee. All subjects gave informed consent.

All subjects were trained to perform horizontal-plane reaching movements, while holding the handle of a planar five-bar, two-link robotic manipulandum (Interactive Motion Technologies, Cambridge, MA), capable of generating torques at each joint. Customized software acquired data from position encoders and tachometers on the manipulandum and generated commands at a rate of 1 kHz. An illustration of the setup is provided in Figure 1. An overhead LCD projector generated visual feedback, including the cursor, start location, and targets, during the reaching task, and displayed movies for movement observation. The projected images were reflected and projected into the plane of reaching via a half-silvered mirror located above the reach workspace. Subjects were seated upright with their upper right arm supported by a sling such that their elbow flexed 90° with his hand holding the manipulandum handle at the start

location. A lamp mounted below the mirror was on during active reaching, allowing subjects vision of their arm, but was off during observation.

Movement task

Throughout the entirety of the task, subjects maintained their grip on the handle of the manipulandum. A yellow circular cursor indicated the veridical location of the manipulandum handle and subject's hand in the task workspace. Movement start location was indicated by a white-outlined circle fixed at the origin of a rectangular coordinate system centered over the workspace. Subjects waited with their hand at the start location until a circular target appeared at one of eight possible locations, evenly distributed on the circle 10 cm about the start location. Subjects were trained to move and stop on the target in the correct time to turn it green. In order to perform a successful reaching movement, subjects were required to stop on the target 750±50 milliseconds after initiating the movement. The target color changed to provide timing feedback: green, successful; red, early; blue, late. Following completion of each movement, the manipulandum returned the handle and subject's hand and arm back to the starting location and posture.

Force channel trials

During a force channel trial, subjects performed a reaching movement to the target as the robotic manipulandum implemented real-time forces on the handle as a stiff spring-damper system,

$$F_{\perp} = -Kx_{\perp} - B\dot{x}_{\perp} \quad (1),$$

where $x_{\perp}$ and $\dot{x}_{\perp}$ denoted the real-time position and velocity components of handle movement perpendicular to a straight-line vector pointing from the start location to the target location, with spring constant K=6000 N/m and a damping constant B=150 Ns/m (Equation 1). The time series of robot-generated clamp forces reflected a mirror image of the subjects' predictive lateral force output. The forces reduced to millimeters the lateral deviation of the manipulandum handle from a straight-line trajectory from start location to the target.

Experiment 1

Subjects were assigned to one of four groups: a Viscous Movement Group (V_{MOV}, n=10), Stiff Movement Group (S_{MOV}, n=10), Viscous Observation Group (V_{OBS}, n=10), and a Stiff Observation Group (S_{OBS}, n=10). Each of these group designations refers to the Learning Block protocol (Movement; Observation) and force field type (Stiff, or position-dependent; Viscous, or velocity-dependent). The experiment task was divided into 3 blocks (Baseline, Learning, Testing) with two 3-minute breaks (Figure 2).

Baseline Block: All subjects first performed 96 reaching movements in the absence of manipulandum-applied forces (null field). All movements were

pseudo-randomly ordered across the 8 target directions, with each target appearing an equal number of times. Pseudo-randomly interspersed among the final 48 null field movements in this block, subjects also performed two force channel movements to each target (16 total). Following the Baseline Block, subjects were given a 3-minute break before continuing with the task.

Learning Block: Movement group subjects performed 192 reaching movements in the presence of either a viscous (V_{MOV} group) or stiff curl field (S_{MOV} group), with forces F_x and F_y,

$$\begin{bmatrix} F_x \\ F_y \end{bmatrix} = K\begin{bmatrix} 0 & 1 \\ -1 & 0 \end{bmatrix}\begin{bmatrix} x \\ y \end{bmatrix} + B\begin{bmatrix} 0 & 1 \\ -1 & 0 \end{bmatrix}\begin{bmatrix} \dot{x} \\ \dot{y} \end{bmatrix} \quad (2),$$

where x and y were the current Cartesian hand position and $\dot{x}$ and $\dot{y}$ were the current Cartesian hand velocity, and the origin of the Cartesian plane lay at the central start location. When exposed to the state-dependent force field, subjects need to produce compensatory forces that mirror the manipulandum-generated forces to move in a straight-line fashion. For the V_{MOV} group, the viscous gain B=21 Ns/m while the stiff gain K=0 N/m for all perturbation trials; for the S_{MOV} group, K=45 N/m and B=0 Ns/m. The viscous and stiff gains were selected to produce similar peak forces (~4.5 N) for typical movements made in each force field. All subjects were given a 3-minute break from the movement task after the first 96 movements, then performed another 96 movements in the same force field condition.

During the Learning Block, observation group subjects did not perform reaching movements. Instead, they watched a movie of a naive actor performing

192 reaching movements with the viscous (V_{OBS} group) or stiff (S_{OBS} group) curl field conditions described above, respectively, with a 3 minute break after watching the first 96 movements. During observation, subjects were instructed to remain motionless, holding the handle at the start location. They were not informed of the content of the movie and only instructed to watch it. The movie they watched was a combination of (1) a movie showing a birds-eye view of an actor's right arm and hand holding the manipulandum and performing reaching movements and (2) a movie showing the actor's hand cursor, start location, and target locations. The combined movie shown during observation was created using Adobe Premier Pro v7.0 software (Adobe Systems Inc.), by cropping, scaling, and overlaying the movies to closely match the typical visual feedback experience of a reaching movement trial.

Testing Block: Following the last trial of the Learning Block, all groups of subjects immediately transitioned to the Testing Block with no break and performed 24 force channel movement trials, one to each target location, pseudo-randomly ordered within each bin of 8 trials.

The blocked experiment design of the current study was largely inspired by Mattar and Gribble (2005), with the intent of replicating their reported learning effect for the V_{OBS} group. However, this implementation does differ from their design in a key aspect in the Learning Block. Subjects in the current study observed another person progressing from naive to experienced in the force field over the course of 192 movements, with a break midway during observation, while in Mattar and Gribble (2005), observers twice watched the first 96

movements of a naive learner training in the force field. We altered this feature so our movement and observation groups experienced parallel training; we cannot restart naïve direct action training after 96 movements. Aside from this difference, the protocol experienced by the V_{OBS} group largely mimicked the conditions used for the viscous force field observation groups in the primary experimental results reported by Mattar and Gribble (2005).

Observation movie actors

Two observation movie actors (Viscous Observation Actor (V_{ACTOR}), female, age 21; Stiff Observation Actor (S_{ACTOR}), female, age 21) had no previous training on the motor task prior to the experiment and experienced the same task design as their respective Movement group. Actors were aware that their movements were being visually recorded by an overhead camera. Due to constraints of using an overhead camera, these actors performed the task with visual feedback provided via a vertically mounted computer screen, and peripheral vision of the arm unoccluded. Except for this difference in feedback presentation, each actor performed the same task as their respective Movement group subjects.

Experiment 2

Following analysis of Experiment 1, we recruited additional subjects for a second Stiff Observation group ($S_{OBS,2}$, n=10). These subjects experienced a modified Learning Block but otherwise identical experimental design as described for Experiment 1. As previously noted, the design for Experiment 1 deviated from that of Mattar and Gribble (2005) as subjects watched movies covering 192 movements instead of twice observing the same sequence of 96 movements. Here, we hypothesized that by twice showing subjects movements depicted early and later training in the stiff force field, we might enhance the learning effect. Instead of observing the full course of training over 192 reaching movements as the original S_{OBS} group, the $S_{OBS,2}$ group twice watched the first 96 reaching movements of the stiff force field movie, with a 3-minute break in between viewings.

Analyses

To facilitate analyses across trials and subjects, we aligned all kinematic and force channel time series at peak speed. Force output was measured as the sign-flipped time series of lateral forces generated by the robot during force channel trials. Adaptation of force output (adapted lateral force profiles) was quantified as the change in lateral forces measured during the Testing Block from the lateral forces measured during the Baseline Block, averaged across 8-movement bins (one movement to each target). By averaging across trials, we measured the overall adaptive effects of the Learning Block and reduced the

effect of trial-to-trial variability and noise. We calculated an adaptation metric for each subject by integrating the adapted lateral force profiles across time.

For each subject, we modeled the degree to which their adapted lateral force output exhibited dependence on movement state by fitting the adapted lateral force profiles as a linear combination of weighted position and velocity signals (Sing et al. 2009),

$$\hat{F}_{\perp} = \hat{K}x_{\parallel} + \hat{B}\dot{x}_{\parallel} \quad (3),$$

where $\hat{F}_{\perp}$ is the modeled time series of lateral forces, $\hat{K}$ and $\hat{B}$ are the modeled stiff and viscous gains, and $x_{\parallel}$ and $\dot{x}_{\parallel}$ are the parallel components of the Cartesian position and velocity signals. Although the implicit target duration was 750ms, to include all data from all movements, we centered kinematic and force output traces at peak hand speed, then included data 500ms before and after the time of the peak.

To better express the magnitude of state-dependent adaptation, we normalized the modeled viscous and stiff gain parameters by dividing by the actual viscous gains B and K to yield the learned velocity-dependence ($\hat{B}/B$) metric and learned position-dependence ($\hat{K}/K$) metrics, respectively. A unity value would reflect a fully learned state-dependence, while a value of zero would reflect no learned state-dependence. Model goodness-of-fit was measured using the variance accounted for (*vaf*) metric,

$$vaf = 1 - \frac{\mathrm{var}(residual)}{\mathrm{var}(data)} \quad (4).$$

All analyses were performed using Matlab (Mathworks, Natick, MA).

298

299 RESULTS

300

301 *Kinematic performance during adaptation*

302

303 To verify that the hand trajectories viewed by Observation group subjects
304 were representative of the positional hand trajectories generated by the
305 Movement group subjects, we compared the mean performance of the
306 movement group subjects and their respective actor shown in the observation
307 movies. We calculated average full time-course positional trajectories from
308 reaching movements in the Learning Block in 8-movement bins, for the Viscous
309 Movement (V_{MOV}) and Stiff Movement (S_{MOV}) group means and the V_{ACTOR} and
310 S_{ACTOR} movie actors. The average trajectory of movie actor movements shown in
311 the observation movies qualitatively mimicked the mean trajectories of the
312 Movement group subjects (Figure 3).

313 We further examined the evolution of movement error, as quantified by
314 perpendicular displacement (p.d.) at peak speed (Figure 3C). We found no
315 significant difference between the viscous movement group and viscous actor in
316 movement error over the first six bins (unbalanced two-way ANOVA, $p > 0.5$,
317 $F_{1,5}=0.28$) and between the stiff movement group and stiff actor (unbalanced two-
318 way ANOVA, $p > 0.8$, $F_{1,5}=0.02$). We did find that the average p.d. at peak
319 speed in the first movement bin was larger in magnitude for the viscous

movement group than the stiff movement group (one-tailed, unpaired two-sample t-test, $p < 0.001$).

Experiment 1: Viscous Movement (V_{MOV}) and Viscous Observation (V_{OBS}) Groups

To establish a baseline level of force output, subjects reached to each target in force channels in the Baseline Block, interspersed with null force field movements. We generated adapted lateral force profiles as the difference in lateral forces measured in force channels in the Testing Block from baseline performance. As a metric of adaptation, we quantified the overall direction and magnitude of adaptation by integrating over the time series of adapted lateral forces, i.e. the area under the curve. Recall that the force fields were designed to push clockwise with respect to the subject's direction of movement (Equation 2). By convention, a positive integrated force indicated that the subject generally pushed more counterclockwise with respect to the target, compensatory for the force field, and a negative integrated lateral force pushed clockwise, or in the same direction as the force field.

We found that following physical practice, the V_{MOV} group subjects, who directly experienced the viscous force field, adapted their lateral force output to oppose the direction of the experienced or observed force field (Figure 4A, integrated force mean with 95% confidence interval=1.37±0.18 Ns), with the adaptation metric significantly greater than zero (one-tailed t-test: $p < 0.001$). The V_{OBS} group subjects, who observed the actor's movements in the same viscous

force field, had a smaller, but also significant, compensatory change in their lateral force output (Figure 4B, 0.10±0.05 Ns; one-tailed t-test: $p = 0.003$). Although differing in overall magnitude of the adaptive response ($p < 0.001$), the temporal profiles, or shapes, of both the V_{MOV} and V_{OBS} responses were strikingly similar, and reminiscent of a bell-shaped velocity profile.

The force field experienced by the V_{MOV} group subjects and the V_{ACTOR} actor, whose movements were observed by the V_{OBS} group subjects, was viscous, or velocity-dependent. Thus, any learned dependence of the adapted force output on velocity would reflect stimulus-appropriate learning of the force field's novel velocity-force mapping. Conversely, any dependence on position signals would indicate stimulus-inappropriate learning. To consider the degree to which adapted lateral force outputs reflected state-dependent dynamics, we regressed the time series of adapted lateral force outputs, averaged over the first 8 Testing Block trials, on the averaged position and velocity time series (Equation 3). As expected, the V_{MOV} group subjects adapted their lateral force outputs with a strong stimulus-appropriate velocity-dependence and negligible stimulus-inappropriate position-dependence. The mean model parameters with 95% confidence intervals across subjects were $\hat{K}$=-0.52±1.86 and $\hat{B}$=13.76±1.31. We normalized the mean velocity-dependent model parameter $\hat{B}$ by the actual force field gain B=21 Ns/m, calculating a mean stimulus-appropriate learned velocity-dependence ($\hat{B}/B$) of 0.665 (Figure 4C). Although the force field was not position-dependent, we also normalized the mean model parameter $\hat{K}$ by the "equivalent" stiff gain of K^*=45 N/m to calculate an equivalent mean learned

position-dependence ($\hat{K}/K^*$) of -0.012; recall, the V_{MOV} group subjects did not experience position-dependent forces. Goodness-of-fit across subjects was measured as variance-accounted-for or *vaf* (w/ 95% CI) of 0.91±0.02. When fitting the model to the V_{MOV} group subject average data, the *vaf* was 0.93. We additionally calculated the contributions of each state-dependent parameter to the overall fit, finding a partial position *vaf* less than 0.01 and partial velocity *vaf* of 0.93, demonstrating that the velocity-dependent component of the model largely contributed to the overall quality of the fit.

Applying the same analysis to the V_{OBS} group subjects, we found that their adapted lateral force outputs also had a significant velocity-dependence and negligible position-dependence, with mean model stiffness and viscosity parameters across subjects of $\hat{K}$=-0.95±1.03 and $\hat{B}$=1.35±0.64. Goodness-of-fit (*vaf*) across subjects was 0.30±0.13. For the V_{OBS} group subjects, we calculated a mean learned velocity-dependence ($\hat{B}/B$) of 0.064 (Figure 4D), which was approximately 9.6% of the mean velocity-dependence for the V_{MOV} group subjects. The equivalent mean learned position-dependence ($\hat{K}/K^*$) was -0.021. Fitting the model to average data across all V_{OBS} group subjects, the model fit (*vaf*) was 0.71. As before, we calculated the contributions of each state-dependent parameter to the overall fit, finding a partial position *vaf* of 0.09 and partial velocity *vaf* of 0.57, again finding that the velocity-dependent component of the model largely explained the quality of fit.

Experiment 1: Stiff Movement (S_{MOV}) and Observation (S_{OBS}) Groups

While both groups who were exposed to the viscous force field, either directly (V_{MOV}) or visually (V_{OBS}), adapted in a stimulus-appropriate, seemingly state-dependent manner, we did not find this to be the case for the first stiff force field observation group (S_{OBS}). Replicating the previously described analyses, we considered how subjects adapted to the stiff, or position-dependent, force field. We found that Stiff Movement (S_{MOV}) group subjects also strongly compensated for the position-dependent curl field and their adapted lateral force profiles reflected learning of the novel position-force mapping (Figure 5A). Calculating the adaptation (integrated force) metric for each subject, we found the S_{MOV} group subjects adapted with a significant compensatory response (mean±95% CI) of 2.16±0.23 Ns (one-tailed t-test: $p < 0.001$). Fitting the state-dependent model to the adapted lateral force output for each subject, we found the S_{MOV} group subjects had a strong and significant dependence on positional signals and a much weaker, though significant, dependence on velocity signals: the mean model parameters with 95% confidence intervals were $\hat{K}$=41.06±6.56 and $\hat{B}$=1.55±0.53, corresponding to a stimulus-appropriate mean learned position-dependence ($\hat{K}/K$) of 0.912 and stimulus-inappropriate equivalent mean learned velocity-dependence ($\hat{B}/B^{*}$) of 0.074 (Figure 5C). Goodness-of-fit (*vaf*) across subjects was 0.97±0.01. Again fitting the model to the average data, we calculated a *vaf* of 0.99, partial position *vaf* of 0.99, and partial velocity *vaf* of 0.02, finding that the position-dependent component largely contributed to the

411 overall fit. Overall, our analysis for the S_{MOV} group subjects found a strongly
412 stimulus-appropriate, position-dependent adaptation of force output, as expected.
413 Unlike the other three groups, the Stiff Observation (S_{OBS}) group subjects
414 did not significantly adapt to compensate for the observed force field (Figure 5B),
415 with integrated force metric of 0.01±0.13 Ns (two-tailed t-test: p = 0.874).
416 Applying the state-dependent model to force outputs of each subject within the
417 S_{OBS} group, the stiff and viscous parameters (mean ± 95% CIM) were $\hat{K}$=-
418 0.15±1.88 (mean $\hat{K}/K$ of -0.003) and $\hat{B}$=0.35±0.65 (mean $\hat{B}/B^*$ of 0.017) (Figure
419 5D), with *vaf* across subjects of 0.25±0.12. Although the model accounted for
420 some variance in the force trace within subjects, the high variability of the stiff
421 and viscous parameter values indicated a lack of consistency across subjects.
422 When fitting the model to average data across all group subjects, the goodness-
423 of-fit was 0.24, with a partial position *vaf* of -0.03, partial velocity *vaf* of 0.27,
424 exhibiting negligible dependence on stimulus-appropriate positional signals.
425
426 *Experiment 2: Modified stiff force field observation protocol ($S_{OBS,2}$) Group*
427
428 We designed Experiment 1 so action and observation subjects
429 experienced parallel training (Figure 2). This protocol, however, deviated from
430 foundational work (Mattar and Gribble 2005) within which observational subjects
431 watched two cycles of 96 movements of training. We saw no consistency in the
432 adapted force outputs and state-dependency in the S_{OBS} group of Experiment 1,

433 so we designed Experiment 2 to replicate more directly the foundational work
434 that provided double exposure to erroneous and learned behavior.

435 We trained an additional ten ($S_{OBS,2}$) subjects on a modified observation
436 task, in which the Training Block twice showed the first 96 movements performed
437 by the S_{ACTOR} movie actor. Unlike the previous S_{OBS} group subjects, we found
438 that the $S_{OBS,2}$ group subjects, who experienced this modified protocol, produced
439 a compensatory adaptive response (Figure 6A) with integrated force of 0.24±0.07
440 Ns (one-tailed t-test: $p<0.001$). As before, we fit the state-dependent model to
441 adapted force outputs for individual subjects in the $S_{OBS,2}$ group. The mean
442 modeled stiffness and viscosity with 95% confidence intervals, were
443 $\hat{K}$=3.27±0.84 and $\hat{B}$=0.86±0.33, with *vaf* of 0.31±0.17. We calculated the mean
444 learned position-dependence ($\hat{K}/K$) of 0.073 and equivalent mean learned
445 velocity-dependence ($\hat{B}/B^{*}$) of 0.041 (Figure 6B), suggesting both a learned
446 position- and velocity-dependence. Fitting the model to data averaged across all
447 group subjects, the *vaf* was 0.86, with a partial position *vaf* of 0.71 and partial
448 velocity *vaf* of 0.23, indicating that over 80% of the variance accounted for within
449 the force channel could be attributed to the time series of position.
450
451 DISCUSSION
452
453 *Observation of perturbed reaches induced adaptive changes in reach dynamics*
454

455 The goal of this study was to determine whether movement observation
456 alone informed the observers of novel environment dynamics at the level of force
457 output and whether observation-driven adaptation of force output was
458 demonstrably dependent on stimulus-specific movement state. Our hypothesis is
459 that haptic learning via observation generates force outputs whose timing
460 approximates forces experienced by the observed actor. This clarification
461 identifies the adaptive system under study. The input is visual, so we
462 characterize kinematics of actor trajectories early and late in training. The
463 system under study, however, is learning of force outputs; the central contribution
464 of our study is a characterization of forces generated by subject who learn about
465 forces only via observation rather than via direct experience. Previous studies
466 found that observers reached more accurately following observation of another
467 person reaching in a novel haptic environment (Mattar and Gribble 2005; Brown
468 et al. 2010), and suggested this learning effect to be due to the acquisition of a
469 neural representation of the haptic environment. However, a similar study of
470 observational learning in which visual feedback was perturbed described a
471 similar adaptive advantage post-observation but absent the aftereffects that are
472 the hallmark of changes in predictive control (Ong and Hodges 2010). Previous
473 haptic studies probed learning by measuring the displacement of positional
474 traces as subjects moved in the force field following observation, an indirect
475 measure of force output that reflected both feedforward and feedback changes.
476 Here, we presented an experimental design that probed learning using an error-
477 clamped force channel and isolated changes in feedforward force output in

observers who never moved in the haptic environment at any point of training, eliminating the influence of testing in the perturbing environment itself. The measured change in lateral force generation reflected subjects' estimation of necessary dynamics to successfully perform a reaching movement following their movement or observational training. Additionally, we trained subjects in different dynamic environments to consider how adaptation depended on movement state. Our results for the subjects who directly experienced viscous and stiff force fields replicated previous descriptions of force output adaptation (Sing et al. 2009; Wagner and Smith 2008) in terms of magnitude and state-dependent profile. Further, our results showed that following observation of another person performing reaching movements perturbed in the direction perpendicular to the hand by velocity- or position-dependent forces, observers exerted compensatory lateral forces that reflected that state-dependence (although more fully for velocity- than for position-dependence). This modest, but significant, change in predictive force output is congruent with the initial reductions in movement curvature reported previously by others (Mattar and Gribble 2005) and suggests that these previously-reported performance gains were due to a feedforward adaptation at the level of execution and force generation.

The results demonstrated by Gribble and colleagues demonstrate that after watching the actor, subjects move in the force field in a slightly more learned fashion. Here we explore additional details of what subjects can learn through observation. The Gribble results show that, as assessed by partial (~15%) reduction of error in reaching, subjects predict that they will need to alter

their motor output. We ask whether this prediction is relatively coarse or relatively fine. With a coarse prediction subjects could make a movement that corrects for the direction of movement, e.g., if a clockwise force field was learned, the subject could move more in the counterclockwise direction. With a finer prediction the subject could counter the temporal details of the forces. Subjects could match the state-dependence of the observed forces, e.g. whether forces depended on hand position or on hand velocity. The latter prediction would suggest that adaptation moved beyond a directional sense (“move more clockwise or counterclockwise”) into a calculation of an appropriate time series of forces. To assess the difference between these two possibilities, we needed the force channel to measure force output throughout the entirety of the movement. We found force generation of the same scale as the Gribble kinematic improvement and with appropriate state dependence.

We found that subjects who observed movements perturbed by a velocity-dependent force field adapted their force output with a temporal profile well-described by a learned scaling of velocity signals, and similarly, position-dependent force field observers' outputs had an increased dependence on positional signals. That observation-driven adaptation reflected the acquisition of a similar stimulus-specific dependence suggested the engagement of feedforward learning mechanisms transforming the visual information acquired during observation into adaptation of reach dynamics. Models explaining force adaptation as expressions of motor primitives dependent on effector position and/or velocity (Thoroughman and Shadmehr 2000; Sing et al. 2009; Hwang et

524 al. 2003) are reflective of the tuning properties of motor neurons (Ashe and
525 Georgopoulos 1994; Moran and Schwartz 1999; Wang et al. 2007) and
526 proprioceptive sensors such as muscle spindle fibers (Prochazka 1999).
527 Observation seems to engage similar neural mechanisms that can encode
528 dynamics in terms of limb states.

529 In human psychophysics, external dynamic loads appear to be learned
530 with respect to intrinsic parameters such as limb state rather than extrinsic
531 variables such as time or external coordinate systems (Shadmehr and Mussa-
532 Ivaldi 1994; Conditt et al. 1997). Generally, visual signals are associated with
533 motor planning, while proprioceptive signals are associated with the computation
534 of joint- and muscle-based motor commands (Sober and Sabes 2003); here,
535 however, visually captured information was transformed into an appropriate
536 muscle-based force output.The force channel clamps trajectories, providing a full
537 time series of human-generated force throughout the reach. Smith and
538 colleagues have built novel insight into timings, and putative state dependencies,
539 of learned forces. We find a parallel to voltage clamping instructive. No real-life
540 experiment is perfect, so there are certainly voltage fluctuations within a clamp.
541 The control of the membrane is sufficient, however, to record a reliable time
542 series of current. Similarly, here we clamp the horizontal component of trajectory
543 not to provide a perfect minimization of displacement, but to record a trace of the
544 generated force. The force channel traces after movement in the fields
545 demonstrate the reliability and appropriateness of this clamp; when subjects
546 push into the wall with a strong force in these trials, there is not generation of

strong vibration, but rather a stable recording of the force via the trajectory clamp.

Proprioception alone may drive updates in feedforward predictions of dynamics and adaptation to haptic environments (Krakauer et al. 1999; Dizio and Lackner 2000; Tong et al. 2002; Scheidt et al. 2005). This seems appropriate since learned dynamics have been shown to be strongly represented in intrinsic-frame, joint coordinates (Shadmehr and Mussa-Ivaldi 1994). Interestingly, studies of deafferented patients suffering from several impaired or unreliable proprioception have found that visual information could be used to both improve the feedforward control and accuracy of unperturbed reaching movements (Ghez et al. 1995) and, recently, to adapt to a haptic environment (Sarlegna et al. 2010). Although deafferented subjects still strongly differ from observers in that they had access to self-generated motor plans, descending motor commands, and other movement-related signals among other aspects, the above studies suggest visual signals can at least partially compensate for the absence of proprioception in motor control and learning. Our subjects, through observation, paralleled computations made by deafferented patients within which visual signals triggered computations typically ascribed to proprioception.

Repeated observation of early perturbed movements induced stronger effect

The observed trajectories have sizeable error only in the earliest stages of training; error is smaller and decreases even more quickly in the position-

570 dependent environment (Figure 3). The complete set of 192 observed trials,
571 therefore, contains observed error only in the first few bins. The delay between
572 this initial learning and eventual force clamping likely underlies the small
573 amplitude of the force trace, although our measured effect is of the same scale
574 as the improvement measured in the Gribble work. Further, we found that the
575 viscous movement group mean adapted more slowly when compared to the stiff
576 movement group mean: the exponential decay rate of error differed between the
577 two groups, with the viscous group decay rate of 0.36 and stiff group decay rate
578 of 0.96 (or a half-life of 1.9 bins versus 0.7 bins). The quick decay of the stiff
579 error indeed likely necessitates the repeated viewing to induce a noticeable force
580 trace. The most direct test of our hypothesis, then, is comparison of traces
581 following observation of velocity- and position-dependent forces. The shapes of
582 the traces clearly differ and significantly depend on the state-dependence of the
583 observed dynamics, providing novel insight into the specificity of forces learned
584 through observation.

585 Although we induced position-dependent force generation in the second
586 stiff observation group, there is lingering state-inappropriate velocity
587 dependence, unlike the clearer single dependence in the velocity observation
588 group. Sing and colleagues established a default mode of early learning of
589 position or velocity dependent forces, within which predicted forces depended on
590 both states. Sing and colleagues further demonstrated through single-trial
591 learning that exposure to stiff forces induced a more mixed dependence of
592 position and velocity in human force output, whereas exposure to viscous forces

induced force output more clearly dependent on velocity than position. Our current finding that observed stiff forces induce a more mixed dependence confirms the Sing et al result and suggests that humans can likely individuate velocity-dependence of environmental forces than position-dependence.

A functional imaging study by Malfait et al. (2010) and behavioral study by Brown et al. (2010) have implicated trajectory curvature of observed reaching movements as a relevant error signal for the adaptive process. In our study, the stronger adaptive effect of the $S_{OBS,2}$ group coincided with the doubled presentation of the more highly curved trajectories from early training and supports the theory that an error signal related to curvature was driving adaptation. Others have suggested that visually sensed perturbation information can lead to awareness and the formation of weaker explicit internal models as opposed to strong gains in implicit knowledge depending on proprioceptive feedback (Hwang et al. 2006). Although Mattar and Gribble (2005) included a distractor to control for explicit strategic learning effects and attention in their experimental design and found no difference in learning effect, Hwang (2006) hypothesized that top-down attentional effects driven by vision could modulate the tuning of the bases underlying subsequent implicit learning. Although in our present study, observers did not directly train in force fields following observation, it is also possible that the observation of additional curved or a greater variety of deviated trajectories resulted in increased salience and attention paid during observation, amplifying some other learning signals derived from observation.

Neural correlates of learning by observing

In non-human primates, passive observation of goal-directed movements is known to activate a subset of premotor and motor neurons known as mirror neurons (Gallese et al. 1996; Rizzolatti et al. 1996; Tkach et al. 2007; Dushanova and Donoghue 2010). Further, mirror-like neurons (Mukamel et al. 2010) and mirror-like facilitation of motor cortex (Stefan et al. 2005; Fadiga et al. 1995) have been described in humans, though the properties of mirror neurons in humans have not been characterized nearly to the degree as in non-human primates (Turella et al. 2009). The characterization of mirror neurons and the mirror system, to date, has relied on broad validations at the behavioral level; hand movements either generated or observed induced similar levels of neural activity. Here, we introduced a finer-grained assay: the acquisition of particular environmental force dependence, indicative of specific learning of dynamics. Our results pose a deeper question of mirror-like dependence: does neurophysiological or imaged activity reflect broad recognition and understanding or precise motoric computation? This distinction could identify putative co-localized processing of observed and generated coordinates and transformations, not just the existence of an effector trajectory. Recent efforts have suggested human motor cortical involvement by interfering with the consolidation of observation-driven learning using rTMS (Brown et al. 2009) and by identifying similar BOLD activation in motor and cerebellar neural areas (Malfait et al. 2010) as during active reach adaptation (Diedrichsen et al. 2005).

Although the roles of a potential human mirror neuron system in motor learning, imitation, and other visuomotor behaviors are not fully understood, this system could underlie a common neural substrate for learning by observing and learning by doing.

In stroke rehabilitation, physical therapy aims to encourage plasticity and reorganization of damaged neural motor circuits, often through intensive, massed physical practice (Patton et al. 2006). Severe deficits in the ability to produce controlled volitional movement can make standard practice-based approaches very challenging (Garrison et al. 2010). Thus, action observation represents an attractive avenue to engage motor regions in impaired patients without requiring active generation of movement (Pomeroy et al. 2005), and hopefully, to rebuild motor function (Ertelt et al. 2007). Here, we provided realistic specificity and impact to this hope, by demonstrating that observation of movement trajectories can train the brain to alter its output of forces, at the level of muscle activity, and with appropriate state dependence.

ACKNOWLEDGEMENTS

We thank D. N. Tomov for technical expertise.

GRANTS

This work was supported by the U.S. National Institutes of Health Grant R01 HD-055851. P. A. Wanda was also supported by the U.S. National Science Foundation IGERT 0548890 through the Cognitive, Computational, Systems Neuroscience Pathway at Washington University in St. Louis.

DISCLOSURES

The authors have declared that no competing interests exist.

AUTHOR CONTRIBUTIONS

PAW KAT conceived and designed the study, PAW GL performed the experiments and analyzed the data, PAW GL KAT interpreted the results, PAW drafted the manuscript, PAW GL KAT edited and approved the manuscript.

672 REFERENCE LIST
673

674 **Ashe J, Georgopoulos AP.** Movement parameters and neural activity in motor
675 cortex and area 5. *Cereb Cortex* 4: 590-600, 1994.
676 **Brown LE, Wilson ET, Gribble PL.** Repetitive transcranial magnetic stimulation
677 to the primary motor cortex interferes with motor learning by observing. *J Cog*
678 *Neurosci* 21: 1013-1022, 2009.
679 **Brown LE, Wilson ET, Obhi SS, Gribble PL**. Effect of trial order and error
680 magnitude on motor learning by observing. *J Neurophysiol* 104: 1409-1416,
681 2010.
682 **Conditt MA, Gandolfo F, Mussa-Ivaldi FA.** The motor system does not learn
683 the dynamics of the arm by rote memorization of past experience. *J Neurophysiol*
684 78: 554-560, 1997.
685 **Diedrichsen J, Hashambhoy Y, Rane T, Shadmehr R.** Neural correlates of
686 reach errors. *J Neurosci* 25(43): 9919-9931, 2005.
687 **Dizio P, Lackner JR**. Congenitally blind individuals rapidly adapt to coriolis force
688 perturbations of their reaching movements. *J Neurophysiol* 84: 2175-2180, 2000.
689 **Donchin O, Francis JT, Shadmehr R**. Quantifying generalization from trial-by-
690 trial behavior of adaptive systems that learn with basis functions: theory and
691 experiments in human motor control. *J Neurosci* 23: 9043-9045, 2003.
692 **Dushanova J, Donoghue J**. Neurons in primary motor cortex engaged during
693 action observation. *Eur J Neurosci* 31: 386-398, 2010.

694 **Ertelt D, Small S, Solodkin A, Dettmers C, McNamara A, Binkofski F,**
695 **Buccino G.** Action observation has a positive impact on rehabilitation of motor
696 deficits after stroke. *NeuroImage* 36:T164-T173, 2007.
697 **Fadiga L, Fogassi L, Pavesi G, Rizzolatti G.** Motor facilitation during action
698 observation: a magnetic stimulation study. *J Neurophysiol* 73: 2608-2611, 1995.
699 **Gallese V, Fadiga L, Fogassi L, Rizzolatti G.** Action recognition in the premotor
700 cortex. *Brain* 119(2): 593-609, 1996.
701 **Garrison KA, Winstein CJ, Aziz-Zadeh L**. The mirror neuron system: a neural
702 substrate of methods in stroke rehabilitation. *Neurorehab Neural Re* 24(5): 404-
703 412, 2010.
704 **Ghez C, Gordon J, Ghilardi MF**. Impairments of reaching movements in
705 patients without proprioception. II. Effects of visual information on accuracy. *J*
706 *Neurophysiol* 73(1): 361-372, 1995.
707 **Hwang EJ, Donchin O, Smith MA, Shadmehr R**. A gain-field encoding of limb
708 position and velocity in the internal model of arm dynamics. *PLoS Biol* 1(2): 209-
709 220, 2003.
710 **Hwang EJ, Smith MA, Shadmehr R**. Adaptation and generalization in
711 acceleration-dependent force fields. *Exp Brain Res* 169: 496-506, 2006.
712 **Hwang EJ, Smith MA, Shadmehr R**. Dissociable effects of the implicit and
713 explicit memory systems learning control of reaching. *Exp Brain Res* 173: 425-
714 437, 2006.
715 **Kawato M.** Internal models for motor control and trajectory planning. *Curr Opin*
716 *Neurobiol* 9(6): 718-727, 1999.

717 **Krakauer JW, Ghilardi MF, Ghez C**. Independent learning of internal models for
718 kinematic and dynamic control of reaching. *Nat Neurosci* 2(11): 1026-1031,
719 1999.

720 **Lackner JR, Dizio P**. Rapid adaptation to Coriolis force perturbations of arm
721 trajectory. *J Neurophysiol* 72: 299-313, 1994.

722 **Malfait N, Valyear KF, Culham JC, Anton JL, Brown LE, Gribble PL.** fMRI
723 activation during observation of others' reach errors. *J Cog Neurosci* 22(7): 1493-
724 1503, 2010.

725 **Mattar AAG, Gribble PL**. Motor learning by observing. *Neuron* 46: 153-160,
726 2005.

727 **Moran DW, Schwartz AB**. Motor cortical representation of speed and direction
728 during reaching. *J Neurophysiol* 82: 2676-2692, 1999.

729 **Mukamel R, Ekstrom AD, Kaplan J, Iacoboni M, Fried I**. Single-neuron
730 responses in humans during execution and observation of actions. *Curr Biol* 20:
731 750-756, 2010.

732 **Oldfield RC**. The assessment and analysis of handedness: the Edinburgh
733 inventory. *Neuropsychologia* 9: 97-113, 1971.

734 **Ong NT, Hodges NJ**. Absence of after-effects for observers after watching a
735 visuomotor adaptation. *Exp Brain Res* 205: 325-334, 2010.

736 **Patton JL, Stoykov ME, Kovic M, Mussa-Ivaldi FA**. Evaluation of robotic
737 training forces that either enhance or reduce error in chronic hemiparetic stroke
738 survivors. *Exp Brain Res* 168(3): 368-383, 2006.

739 **Pomeroy VM, Clark CA, Miller JSG, Baron J-C, Markus HS, Tallis RC.** The
740 potential for utilizing the "mirror neurone system" to enhance recovery of the
741 severely affected upper limb early after stroke: a review and hypothesis.
742 *Neurorehab Neural Re* 19:4-13, 2005.
743 **Prochazka A**. Quantifying proprioception. *Prog Brain Res* 123: 133-142, 1999.
744 **Rizzolatti G, Fadiga L, Fogassi L, Gallese V**. Premotor cortex and the
745 recognition of motor actions. *Cogn Brain Res* 3:131-141, 1996.
746 **Sarlegna FR, Malfait N, Bringoux L, Bourdin C, Vercher JL**. Force-field
747 adaptation without proprioception: Can vision be used to model limb dynamics?
748 *Neuropsychologia* 48(1): 60-67, 2010.
749 **Scheidt RA, Conditt MA, Secco EL, Mussa-Ivaldi FA**. Interaction of visual and
750 proprioceptive feedback during adaptation of human reaching movements. *J*
751 *Neurophysiol* 93: 3200-3213, 2005.
752 **Scheidt RA, Reinkensmeyer DJ, Conditt MA, Rymer WZ, Mussa-Ivaldi FA**.
753 Persistence of motor adaptation during constrained multi-joint, arm movements. *J*
754 *Neurophysiol* 84: 853-862, 2000.
755 **Shadmehr RA, Mussa-Ivaldi FA.** Adaptive representation of dynamics during
756 learning of a motor task. *J Neurosci* 14: 3208-3224, 1994.
757 **Shadmehr RA, Smith MA, Krakauer JW.** Error correction, sensory prediction,
758 and adaptation in motor control. *Annu Rev Neurosci* 33: 89-108, 2010.
759 **Sing GC, Joiner WM, Nanayakkara T, Brayanov JB, Smith MA**. Primitives for
760 motor adaptation reflect correlated neural tuning to position and velocity. *Neuron*
761 64: 575-589, 2009.

762 **Smith MA, Ghazizadeh A, Shadmehr R**. Interacting adaptive processes with
763 different timescales underlie short-term motor learning. *PLoS Biol* 4: 1035-1043,
764 2006.
765 **Sober SJ, Sabes PN**. Multisensory integration during motor planning. *J Neurosci*
766 23(18): 6982-6992, 2003.
767 **Stefan K, Cohen LG, Duque J, Mazzocchio R, Celnik P, Sawaki L,**
768 **Ungerleider L, Classen J.** Formation of a motor memory by action observation.
769 *J Neurosci* 25(41): 9339-9346, 2005.
770 **Thoroughman KA, Shadmehr R**. Electromyographic correlates of learning an
771 internal model of reaching movements. *J Neurosci* 19: 8573-8588, 1999.
772 **Thoroughman KA, Shadmehr R**. Learning of action through adaptive
773 combination of motor primitives. *Nature* 407: 742-747, 2000.
774 **Thoroughman KA, Taylor JA**. Rapid reshaping of human motor generalization.
775 *J Neurosci* 25: 8948-8953, 2005.
776 **Tkach D, Reimer J, Hatsopoulos NG**. Congruent activity during action and
777 action observation in motor cortex. *J Neurosci* 27(48): 13241-13250, 2007.
778 **Tong C, Wolpert DM, Flanagan JR**. Kinematics and dynamics are not
779 represented independently in motor working memory: evidence from an
780 interference study. *J Neurosci* 22(3): 1108-1113, 2002.
781 **Turella L, Pierno AC, Tubaldi F, Castiello U**. Mirror neurons in humans:
782 consisting or confounding evidence? *Brain Lang* 108:10-21, 2009.
783 **Wagner MJ, Smith MA**. Shared internal models for feedforward and feedback
784 control. *J Neurosci* 28: 10663-10673, 2008.

785 **Wang W, Chan SS, Heldman DA, Moran DW**. Motor cortical representation of
786 position and velocity during reaching. *J Neurophysiol* 97: 4258-4270, 2007.
787 **Wei K, Wert D, Kording K**. The nervous system uses nonspecific motor learning
788 in response to random perturbations of varying nature. *J Neurophysiol* 104:
789 3053-3063, 2010.
790
791

792 FIGURE CAPTIONS

793

794 FIG. 1. Apparatus, observation movie, and force channel. A. Illustration of the
795 experimental apparatus. Subjects were trained to grip the handle of a robotic
796 manipulandum and perform reaching movements. Visual task feedback was
797 displayed in the plane of reaching via an overhead projector and mirrors. B. Still
798 frame taken from a movie shown to observation group subjects during the
799 Learning Block, showing an actor's arm performing a reaching movement with
800 visual feedback overlaid. C. Illustration of force channel movement. The robotic
801 manipulandum generated forces to cancel lateral forces produced by the subject,
802 restricting the cursor along a straight-line path from the start location to the target
803 location.

804

805 FIG. 2. Task design. Five groups of subjects performed a blocked-design
806 reaching task. During the Baseline Block, subjects from all groups were trained
807 on a baseline condition, with no force field present during 96 reaching
808 movements, and with interspersed force channel movements (2 to each target).
809 During the Learning Block, subjects performed (movement groups) or watched
810 (observation groups) 192 reaching movements in the presence of their respective
811 state-dependent force field. Note that Observation Group II watched the first 96
812 movements performed by a naive actor twice, for a total of 192 trials. During the
813 Testing Block, all subjects performed 24 force channel movements (3 to each
814 target).

815

816 FIG. 3. Hand trajectories, averaged over 8-trial bins in the Learning Block. For
817 each force field type, the mean Movement group (brown) performance is
818 compared to the respective actor performance viewed by Observation group
819 subjects (orange). Here, the first bin of movements (Bin 1: 1-8, solid), second bin
820 (Bin 2: 9-16, dashed), and mid-training bin (Bin 12: 89-96, dotted) are averaged
821 and plotted. Mean kinematics were similar for each force field type. A. Viscous
822 Movement (V_{MOV}) Group and the Viscous Observation Actor (V_{ACTOR}). B. Stiff
823 Movement (S_{MOV}) Group and the Stiff Observation Actor (S_{ACTOR}). C. Movement
824 error across 8-trial bins. For the Viscous Movement and Stiff Movement groups,
825 movement error was quantified by the mean perpendicular displacement at peak
826 speed for bins 1 to 12 (mean ± 95% CI).

827

828 FIG. 4. Adapted force output for viscous force field groups and model fits. A, B.
829 Adapted lateral force profiles with shaded 95% confidence intervals (CI) across
830 subjects, with state-dependent model fits overlaid. Adapted profiles are
831 calculated as the difference between the Testing block profile and the Baseline
832 block profile, averaged over the first 8 force channel movements of the Testing
833 Block (one to each target). The V_{MOV} group (A) and V_{OBS} Group (B) mean profiles
834 both showed significant changes from baseline. B, inset. Single trial force trace
835 (grey) and mean force trace (black) for an individual V_{OBS} subject (#3). Subject
836 had normalized parameter values of 0.01 ($\hat{K}/K^*$) and 0.10 ($\hat{B}/B$). C, D.

Respective bar plots show the normalized mean model state-dependent parameter values with 95% CI across subjects (B, V_{MOV}, n=10; D, V_{OBS}, n=10).

FIG. 5. Adapted force output for stiff force field groups and model fits. A, B. Adapted lateral force profiles with shaded 95% CIs, with state-dependent model fits. The S_{MOV} group (A) mean profile had a significant change from baseline, and the S_{OBS} Group (B) did not have a significant change from baseline. C, D. Respective bar plots show the normalized mean model state-dependent parameter values with 95% CI (B, S_{MOV}, n=10; D, S_{OBS}, n=10).

FIG. 6. Adapted force output for stiff force field observation group 2 and model fit. $S_{OBS,2}$ group subjects watched the first set (1-96) of stiff force field movements twice, instead of the full training span of 192 trials. A. Adapted lateral force profiles with shaded 95% CIs, with state-dependent model fits. The $S_{OBS,2}$ group mean adapted force profile had a significant change from baseline. A, inset. Single trial force trace (grey) and mean force trace (black) for an individual $S_{OBS,2}$ subject (#2). Subject had normalized parameter values of 0.08 ($\hat{K}/K$) and 0.02 ($\hat{B}/B^*$). B. The bar plot of normalized mean model state-dependent parameters with 95% CI (n=10).

A

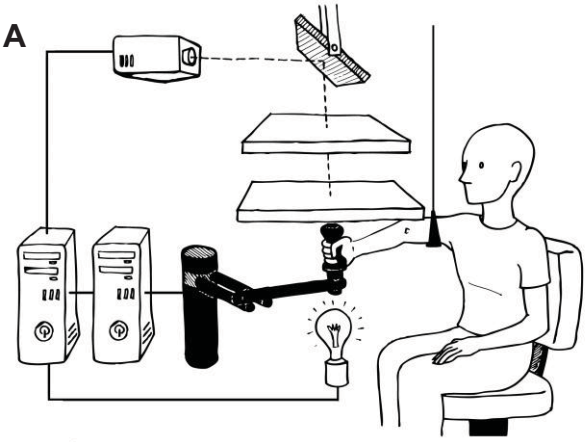

B

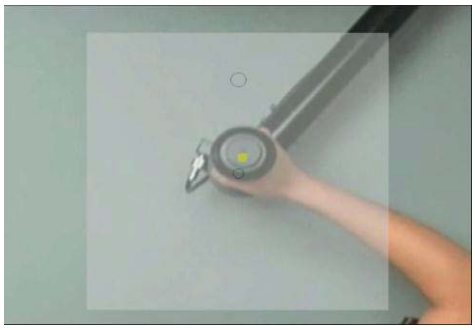

C

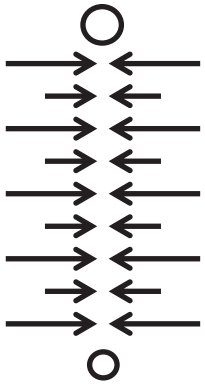

	Movement Groups S_{MOV} (n=10) V_{MOV} (n=10)	**Observation Groups** S_{OBS} (n=10) V_{OBS} (n=10)	**Observation Group 2** $S_{OBS,2}$ (n=10)
Baseline	**Perform** no-force movements (96), and force channel movements (16)		
Learning	**Perform** force field movements (192)	**Observe** force field movements (1 to 192)	**Observe** force field movements (1 to 96) x 2
Testing	**Perform** force channel movements (24)		

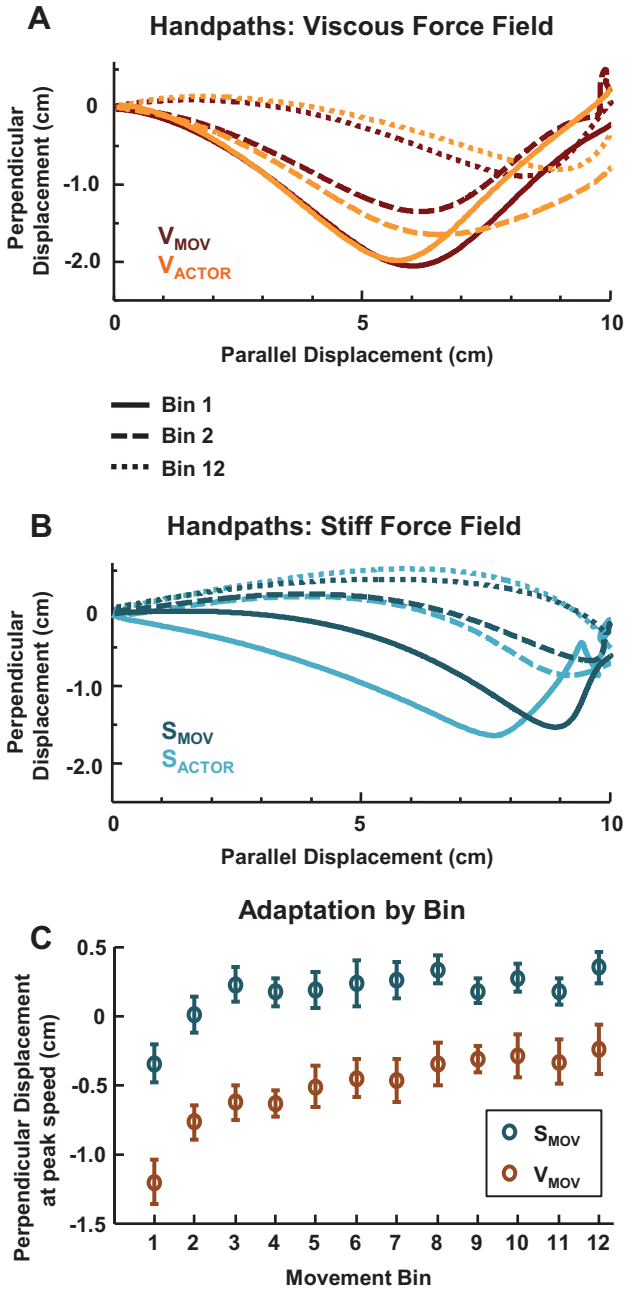
A
Handpaths: Viscous Force Field
Perpendicular Displacement (cm)
0
-1.0
-2.0
0
5
10
Parallel Displacement (cm)
V_MOV
V_ACTOR
Bin 1
Bin 2
Bin 12
B
Handpaths: Stiff Force Field
Perpendicular Displacement (cm)
0
-1.0
-2.0
0
5
10
Parallel Displacement (cm)
S_MOV
S_ACTOR
C
Adaptation by Bin
Perpendicular Displacement at peak speed (cm)
0.5
0
-0.5
-1.0
-1.5
1
2
3
4
5
6
7
8
9
10
11
12
Movement Bin
S_MOV
V_MOV

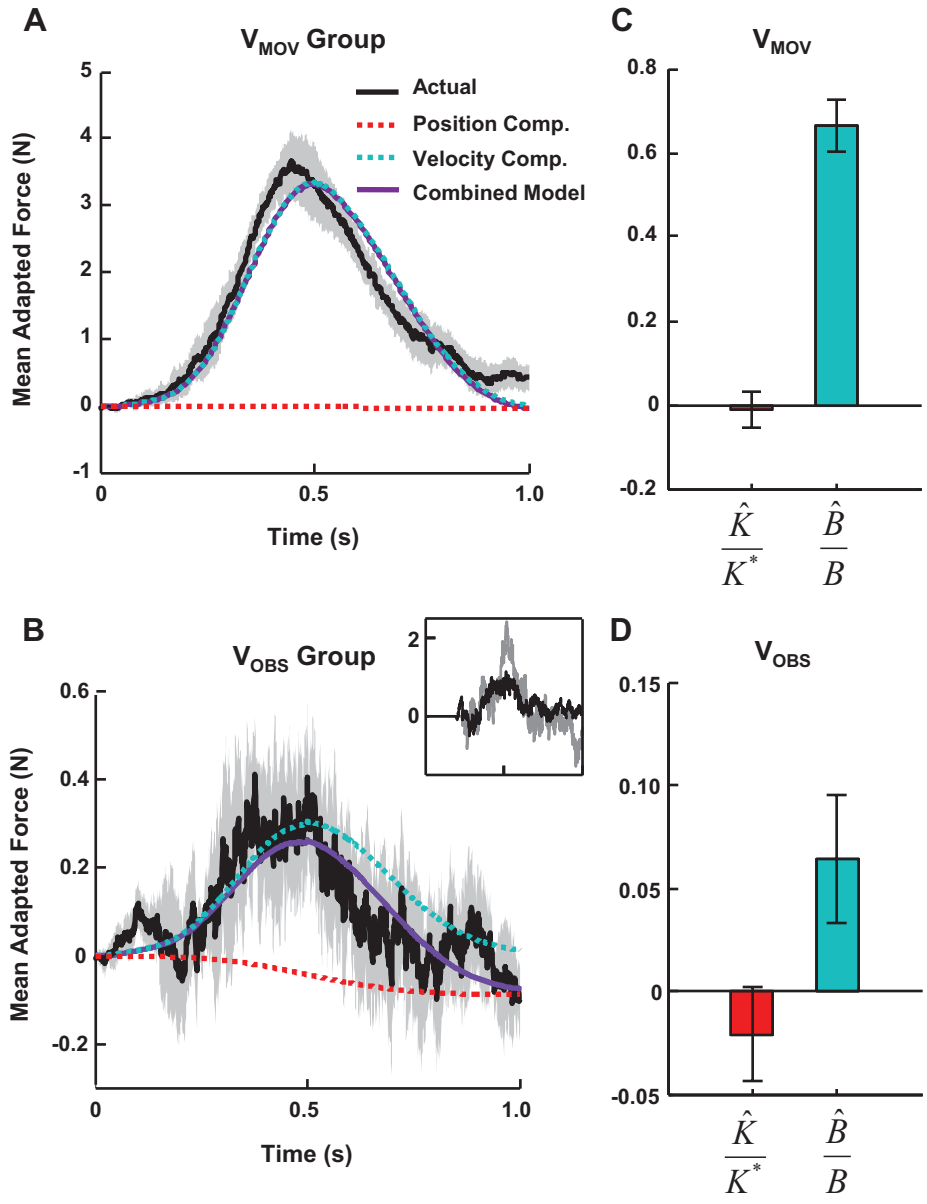
A
V_MOV Group
Actual
Position Comp.
Velocity Comp.
Combined Model
Mean Adapted Force (N)
Time (s)
C
V_MOV
B
V_OBS Group
Mean Adapted Force (N)
Time (s)
D
V_OBS

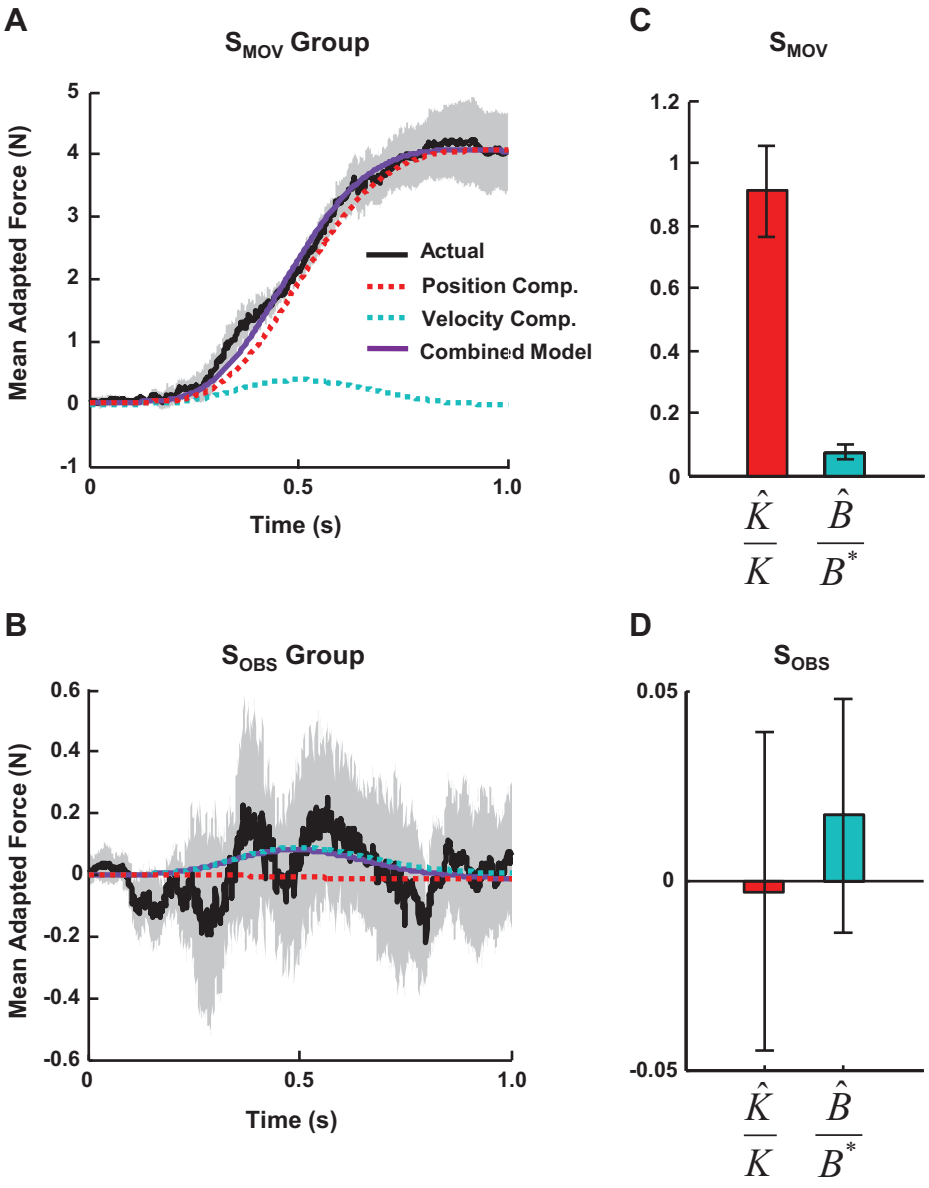
A
S_MOV Group
Mean Adapted Force (N)
Time (s)
Actual
Position Comp.
Velocity Comp.
Combined Model
B
S_OBS Group
Mean Adapted Force (N)
Time (s)
C
S_MOV
D
S_OBS

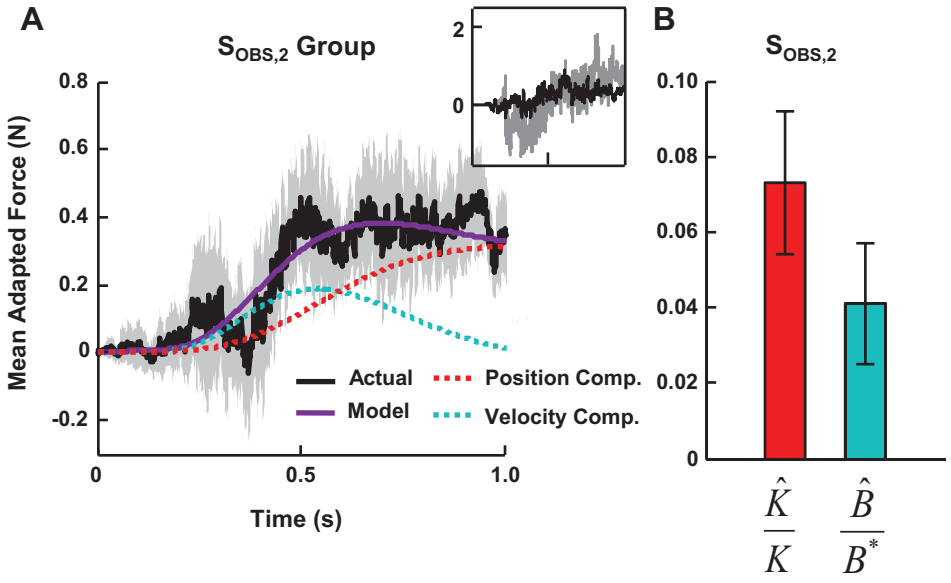
A
$S_{OBS,2}$ Group
Mean Adapted Force (N)
0.8
0.6
0.4
0.2
0
-0.2
0
0.5
1.0
Time (s)
2
0
Actual
Model
Position Comp.
Velocity Comp.
B
$S_{OBS,2}$
0.10
0.08
0.06
0.04
0.02
0
$\frac{\hat{K}}{K}$
$\frac{\hat{B}}{B^*}$